TISSUE ENGINEERING: Part A
Volume 20, Numbers 1 and 2, 2014

DOI: 10.1089/ten.tea.2012.0687

Sequential Platelet-Derived Growth Factor–Simvastatin Release Promotes Dentoalveolar Regeneration

Po-Chun Chang, DDS, PhD,[1,2] Li Yen Chong, MSc,[2] Alex S.M. Dovban, BDSc, MS,[2]
Lum Peng Lim, BDSc, MS,[2] Jason C. Lim, BEng,[3]
Mark Yen-Ping Kuo, DDS, PhD,[1] and Chi-Hwa Wang, PhD[4]

Objectives: Timely augmentation of the physiological events of dentoalveolar repair is a prerequisite for the optimization of the outcome of regeneration. This study aimed to develop a treatment strategy to promote dentoalveolar regeneration by the combined delivery of the early mitogenic factor platelet-derived growth factor (PDGF) and the late osteogenic differentiation factor simvastatin.
Materials and Methods: By using the coaxial electrohydrodynamic atomization technique, PDGF and simvastatin were encapsulated in a double-walled poly(D,L-lactide) and poly(D,L-lactide-*co*-glycolide) (PDLLA–PLGA) microspheres in five different modes: microspheres encapsulating bovine serum albumin (BB), PDGF alone (XP), simvastatin alone (SB), PDGF-in-core and simvastatin-in-shell (PS), and simvastatin-in-core and PDGF-in-shell (SP). The microspheres were characterized using scanning electronic microscopy, and the *in vitro* release profile was evaluated. Microspheres were delivered to fill large osteotomy sites on rat maxillae for 14 and 28 days, and the outcome of regeneration was evaluated by microcomputed tomography and histological assessments.
Results: Uniform 20-μm controlled release microspheres were successfully fabricated. Parallel PDGF–simvastatin release was noted in the PS group, and the fast release of PDGF followed by the slow release of simvastatin was noted in the SP group. The promotion of osteogenesis was observed in XP, PS, and SP groups at day 14, whereas the SP group demonstrated the greatest bone fill, trabecular numbers, and thickest trabeculae. Bone bridging was evident in the PS and SP group, with significantly increased osteoblasts in the SP group, and osteoclastic cell recruitment was promoted in all bioactive molecule-treated groups. At day 28, osteogenesis was promoted in all bioactive molecule-treated groups. Initial corticalization was noted in the XP, PS, and SP groups. Osteoblasts appeared to be decreased in all groups, and significantly, a greater osteoclastic cell recruitment was noted in the SB and SP groups.
Conclusions: Both PDGF and simvastatin facilitate dentoalveolar regeneration, and sequential PDGF–simvastatin release (SP group) further accelerated the regeneration process through the enhancement of osteoblastogenesis and the promotion of bone maturation.

Introduction

One of the major challenges in dental implantology is the deficiency of the alveolar bone, which is necessary to provide an adequate implant support, and numerous efforts have concentrated on augmenting the alveolar bone with bone substitute grafting or regenerative membranes.[1] Recently, bioactive molecules, such as platelet-derived growth factor (PDGF), bone morphogenetic protein (BMP), and simvastatin, were implemented in preclinical models and demonstrated a significant acceleration of dentoalveolar repair.[2,3] However, the clinical efficiency was still not in line with the preclinical findings, especially in the severely atrophic alveolar bone ridge.[4] Because bone repair is the consequence of the coordination of various growth factors,[5,6] delivering multiple biomolecules in accordance with their biological effects appears to be a logical strategy to achieve optimal dentoalveolar regeneration.

Recent studies have demonstrated that the combined delivery of biomolecules, such as BMP plus insulin-like growth factor (IGF),[7] or BMP plus vascular endothelial growth factor,[8] showed superior regenerative effects in bone compared with single biomolecule delivery through the amplification of osteogenic, mitogenic, and angiogenic effects. However,

[1]Graduate Institute of Clinical Dentistry, School of Dentistry, National Taiwan University, Taipei, Taiwan.
[2]Faculty of Dentistry, National University of Singapore, Singapore, Singapore.
[3]Singapore Bioimaging Consortium (SBIC), Agency for Science, Technology, and Research (A*STAR), Singapore, Singapore.
[4]Department of Chemical and Biomolecular Engineering, Faculty of Engineering, National University of Singapore, Singapore, Singapore.

the discrepancies of the treatment outcome still exist, implicating that the harmonization of dose, ratio, and timely release of biomolecules may play a determinative role in bone regeneration.[9] It is of interest to develop a matrix that is capable of controlling the release sequence of dual or multiple biomolecules. In this regard, hybrid scaffolds, such as gelatin microparticle-encapsulated hydrogels,[10] glutaraldehyde-crosslinked gelatin layers,[11] and porous polymer microsphere-encapsulated scaffold,[9] have been employed to coordinate the release sequence of dual biomolecules for the purpose of tissue regeneration.

A double-layered poly(D,L-lactide) and poly(D,L-lactide-*co*-glycolide) (PDLLA–PLGA) microsphere, which is capable of encapsulating two biomolecules based on the variability of hydrophilicity, had been previously developed from our group and had demonstrated acceptable biocompatibility.[12] With the encapsulation of PDGF, a mitogen that modulates cell proliferation in the early stage,[13] and simvastatin, a differentiation factor that induces osteogenesis in the later stage,[14] these microspheres demonstrated improved cellular variability, reduction of inflammation, and resistance to the heat-induced osteonecrosis.[12,15] In this study, we aimed to establish a treatment strategy through the dual delivery of PDGF–simvastatin utilizing PDLLA–PLGA microspheres to facilitate dentoalveolar regeneration.

Materials and Methods

Microsphere fabrication

Human recombinant PDGF-BB was acquired from Luitpold Pharmaceuticals (Wilmington, DE), and purified simvastatin was purchased from Sigma-Aldrich Co. LLC (St. Louis, MO). The microspheres were fabricated by the coaxial electrohydrodynamic atomization technique (CEHDA) as previously described.[12] The matrix solutions were formulated by dissolving 10% PDLLA (Mw: 24,300–75,000) and 10% PLGA (50:50, Mw: 31,300–43,500) (Lactel Absorbable Polymers, Pelham, AL) in dichloromethane solution respectively, and the resulting solutions were transferred to a coaxial needle (inner channel: PDLLA; outer channel: PLGA) controlled by two programmable syringe pumps and an electrical field. One milligram hydrophobic biomolecules (simvastatin) were dissolved in the matrix solution directly, whereby 1 mg hydrophilic agents (PDGF or bovine serum albumin [BSA]) were dissolved in deionized water and transferred to the corresponding matrix solution. Five types of PDLLA–PLGA microspheres were fabricated: (i) BSA-in-core and BSA-in-shell (BB), (ii) PDGF-in-shell (XP), (iii) simvastatin-in-core and BSA-in-shell (SB), (iv) PDGF-in-core and simvastatin-in-shell (PS), and (v) simvastatin-in-core and PDGF-in-shell (SP). Based on our previous study, it would achieve about 5.5–7.4 pg PDGF or simvastatin encapsulated in the core compartment of each microsphere, and 4.5–5.9 pg in the shell compartment.[15]

The size and surface morphology of the microspheres were examined by scanning electron microscopy, and the core–shell structure was confirmed by the distribution of coumarin-6 under a confocal laser scanning microscope. The encapsulation efficiency of bioactive molecules within the microspheres was examined by dissolving the microspheres in dichloromethane and phosphate-buffered saline (PBS) with centrifugation at 9000 rpm. The *in vitro* release profiles of PDGF and simvastatin were examined by loading the microspheres in PBS under consistent shaking (120 rpm) at 37°C and collecting the incubated medium at days 1, 3, 5, 7, 10, and 14. The concentrations of PDGF and simvastatin in the medium were evaluated by ELISA and high-performance liquid chromatography, respectively.

Study design and animal model

Seventy-two 4-week-old (weight ~75–90 g) male Sprague-Dawley rats were utilized in this study following the protocol 057/10 approved by the Institutional Animal Care and Use Committee of the National University of Singapore (NUS), and the sample size was determined by Power Analysis based on a relevant study.[15] All the surgical procedures were performed under the generalized coverage of ketamine (70 mg/kg) and xylazine (10 mg/kg). The maxillary first molar (M1) from a randomly selected side was surgically removed using a dental explorer from each animal. After 4 weeks of socket healing, a uniform osteotomy (2.6 mm diameter and 1 mm depth, with 0.6 mm to the middle of mesial aspect of M2) was created in the post-extraction ridge of M1 using a customized low-speed drill (2.6 mm diameter of the cutting surface with the design of vertical stop at 1 mm depth and 0.6 mm noncutting collar to ensure the consistent distance to M2) under 3000 rpm with copious normal saline irrigation. The osteotomy sites were randomly assigned to six modes based on the treatments: filled with microspheres encapsulating BB, SB, XP, SP, and PS, respectively, or unfilled with microspheres (Ctrl). The wound was closed with a cyanoacrylate gel (Histoacryl®; TissueSeal LLC, Ann Arbor, MI). Animals underwent antibiotics coverage (268 mg/mL ampicillin in the drinking water) for 7 days and were euthanized to harvest the maxillae at days 14 and 28 ($n = 6$ per mode per time point).

Microcomputed tomography

The harvested maxillae were examined by a Siemens Inveon CT System (Siemens Healthcare, Erlangen, Germany) with an 80 W tungsten anode, 30–80-kVp variable focus X-ray source, and a 165-mm detector. The images were reconstructed using the Shepp-Logan algorithm to achieve an effective pixel size of 19 microns, and the threshold of the image was determined by a standardized local edge detection algorithm.[16] The entire osteotomy site was selected as the region of interest (ROI), which is 2.6 mm diameter and 1 mm depth with 0.6 mm to the middle of mesial aspect of M2, and the micromorphometric bone parameters, including relative bone volume (BV/TV), bone mineral density (BMD), tissue mineral density (TMD), trabecular thickness (Tb.Th), trabecular separation (Tb.Sp), and trabecular number (Tb.N), were separately calculated for each ROI using the CTAn software (Skyscan, Kontich, Belgium).

Histological analysis

After microcomputed tomography (micro-CT) scanning, the specimens were decalcified with 12.5% EDTA (pH 7.4) for 3 weeks. A sagittal section that crossed the midpoints of the maxillary second (M2) and third molars (M3) was selected, and the specimens were then embedded in paraffin and sectioned to 5 μm thickness. Hematoxylin and eosin

(Polysciences, Inc., Warrington, PA) stains were performed for the histological observation and the quantification of defect bone fill and osteoblasts. As the osteoclasts on the newly formed bone could be an indicator of bone remodeling,[17] tartrate-resistant acid phosphatase (TRAP), a biomarker of active osteoclasts, was analyzed using a Leukocyte Acid Phosphatase kit (Sigma-Aldrich Co. LLC). All of the histological and histochemical images were acquired utilizing a Leica DMD108 system (Leica Microsystems GmbH, Wetzlar, Germany).

Histomorphometric measurements were performed using ImageJ software (NIH, Bethesda, MD), and the region of the defect was selected in accordance with the ROI of the correspondent plane of the micro-CT imaging. The percentage of defect filled with newly formed bone was assessed under 40× magnification. The averaged numbers of osteoblasts and TRAP(+) cells were evaluated in five randomly selected areas within 25 μm from the surface of the newly formed bone in each osteotomy site under 400× magnification.

Statistical analysis

All data are presented as the mean ± standard deviation, and the statistical analysis was performed by GraphPad Prism software (La Jolla, CA). The differences between the control (Ctrl and BB groups) and bioactive molecule treatments were compared by one-way ANOVA followed by Tukey's *post hoc* test, with a *p*-value of less than 0.05 considered to be statistically significant.

Results

Characterization of the microspheres

The distinct dual-layered microspheres were successfully fabricated with a uniform size (18–21 μm in diameter), regardless of the carried molecules (Fig. 1A). The encapsulation efficiency—the percentage of bioactive molecules successfully encapsulated in the correspondent compartment of the microsphere—was 50%–80% for the shell compartment and 80%–96% for the core compartment (Table 1).

The *in vitro* release profile varied according to the type of molecular distribution in the microspheres. In the XP design, ~60% of the PDGF was released within the first 3 days, and the release was nearly completed at day 10 (Fig. 1B). The SB design, however, demonstrated a slow release profile, with less than 50% released at day 14 (Fig. 1C). In the PS design, the release rates of PDGF and simvastatin were parallel, with 60% of the molecules released at day 10 (Fig. 1D). The SP design demonstrated a sequential release profile, which is characterized by a fast release of PDGF, similar to the XP design, and a slow release of simvastatin, similar to the SB design (Fig. 1E).

Micro-CT assessments

Limited osteogenesis was noted in the Ctrl and BB groups throughout the observation period (Fig. 2). Osteogenesis was apparently greater in the sites treated with bioactive molecules (PDGF or simvastatin) at day 14, and significantly

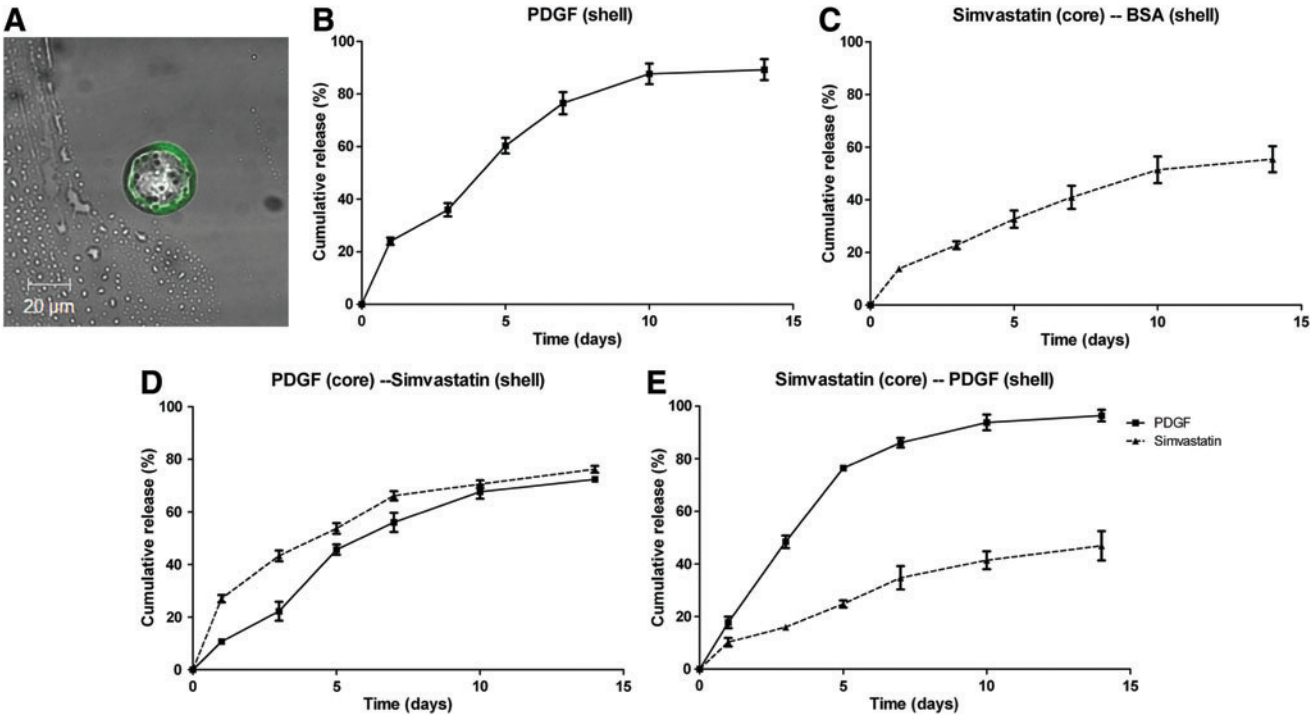

FIG. 1. Characterization of PDLLA–PLGA microspheres. **(A)** A distinct core–shell structure was demonstrated by encapsulating coumarin-6 to the outer compartment of the microsphere, 1000×. **(B–E)** The *in vitro* release profiles of **(B)** XP, PDGF (shell); **(C)** SB, simvastatin (core)/BSA (shell); **(D)** PS, PDGF (core)/simvastatin (shell); and **(E)** SP, simvastatin (core)/PDGF (shell) microspheres. PDGF, platelet-derived growth factor; BSA, bovine serum albumin; PDLLA–PLGA, poly(D,L-lactide) and poly(D,L-lactide-*co*-glycolide). Color images available online at www.liebertpub.com/tea

Table 1. Particle Size and Encapsulation Efficiency of the Microspheres

Name of specimen		*BB BSA (core)/ BSA (shell)*	*SB simvastatin (core)/BSA (shell)*	*XP PDGF (shell)*	*PS PDGF (core)/ simvastatin (shell)*	*SP simvastatin (core)/PDGF (shell)*
Particle size (μm)		18.1 ± 1.9	20.9 ± 1.5	18.6 ± 1.0	19.8 ± 1.3	18.8 ± 0.8
Encapsulation efficiency (%)	Core	60.0 ± 2.2	96.2 ± 3.5	NA	93.8 ± 2.6	84.5 ± 2.5
	Shell		63.5 ± 0.2	53.9 ± 1.1	83.2 ± 2.7	60.3 ± 2.2

PDGF, platelet-derived growth factor; BSA, bovine serum albumin; NA, not available.

greater osteogenesis with initial bridging of bone within osteotomy sites was noted in the PS and SP groups (Fig. 2, left panel). The density of neogenic bone appeared to increase at day 28 in all specimens (Fig. 2, right panel).

The quantitative measurements demonstrated greater BV/TV and TMD in sites treated with bioactive molecules (i.e., PDGF, simvastatin, or combination) relative to controls (Ctrl and BB groups), and a significant difference from the controls was noted in the SP group at day 14 (Fig. 3A, B). Tb.Th and Tb.N were also significantly enhanced in the PS and SP groups at day 14 (Fig. 3C, D). At day 28, all bioactive molecule-treated sites consistently revealed greater BV/TV, TMD, Tb.Th, and Tb.N values relative to controls, and significant differences from controls were noted in the SB, XP, and SP groups. All the micro-CT parameters in the XP group appeared to reach the greatest level, equivalent to that of the SP group at day 28 (Fig. 3). There was no obvious difference in the BMD among all groups at both time points, and Tb.Sp was slightly and insignificantly decreased in the PS and SP groups at day 14 (data not shown).

Descriptive histology

At day 14, the osteotomy site was mainly occupied by fibrous tissues with scattered primitive bone apposition on the border in the Ctrl group. The pattern of osteogenesis was similar in the BB group, with residual microspheres surrounded by foreign body giant cells and mild inflammatory cell infiltration. Relatively fewer residual microspheres with greater amounts of the thin trabecular bony structure were noted in the XP and SB groups. In the SP and PS groups, the osteotomy sites appeared to be largely occupied by a thicker trabecular bone, and the reversal lines within the newly formed bone could only be observed in the PS and SP groups (Fig. 4A).

At day 28, residual microspheres were still noted in most microsphere-treated sites, but the amount of microspheres appeared to be greatly reduced. Compared with day 14, the thickness of trabecular bone appeared to increase in all groups by day 28 (except the PS group), whereas reversal lines within the newly formed bone matrix were noted in XP,

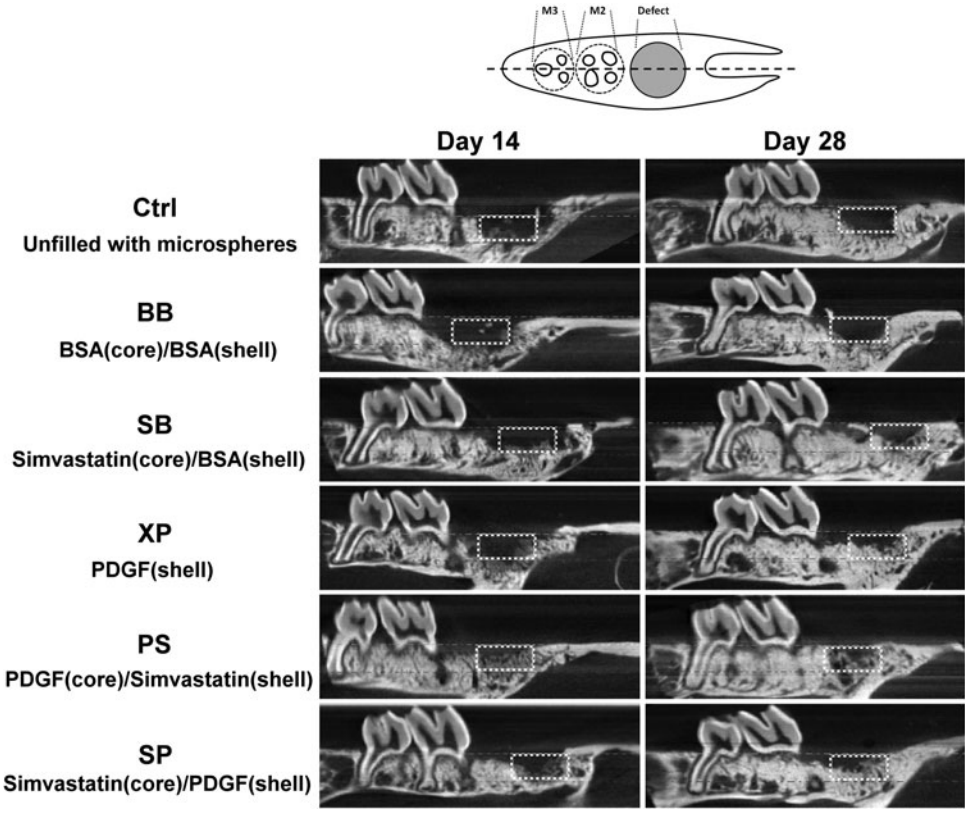

FIG. 2. Pattern of dento-alveolar regeneration from micro-CT imaging. A sagittal slice crossing the midline of the maxillary molars was selected (dashed line in the upper panel) from one representative specimen in each treatment group at day 14 (left panel) and day 28 (right panel). The dashed boxes indicate the region of osteotomy. Micro-CT; microcomputed tomography.

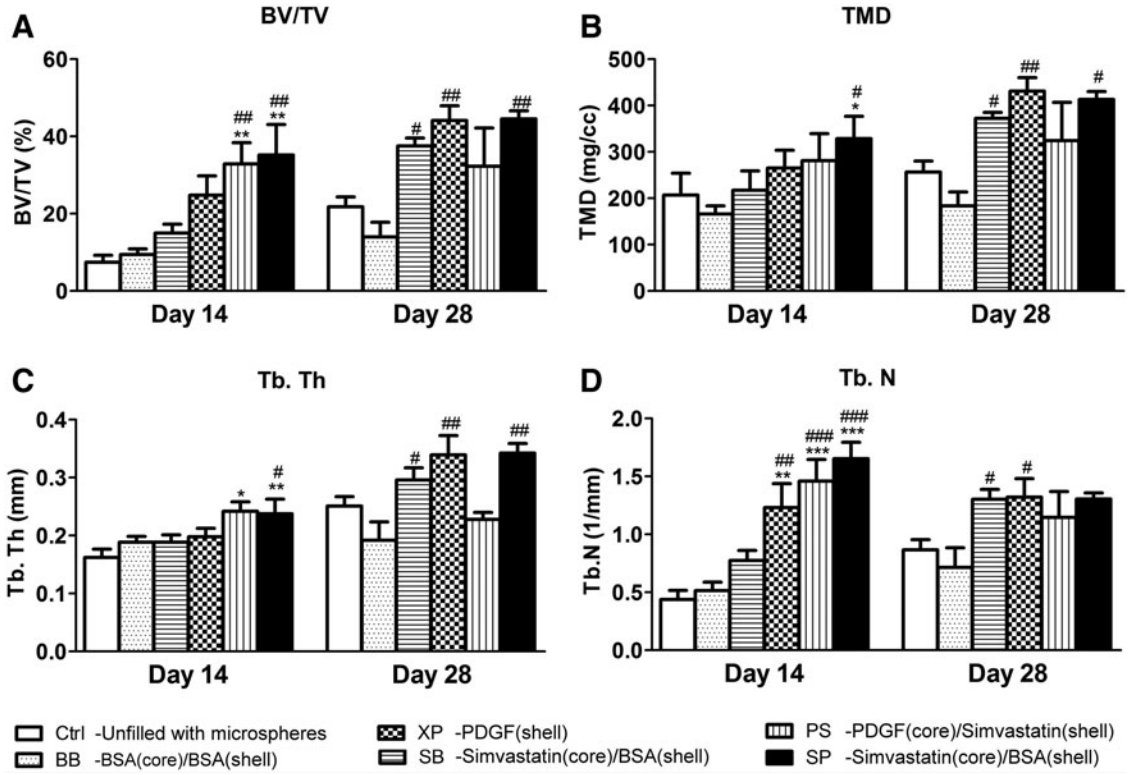

FIG. 3. Quantitative assessments of micro-CT imaging. **(A)** BV/TV; **(B)** TMD; **(C)** Tb.Th; **(D)** Tb.N. (Data are expressed as mean ± standard deviation, and differences between groups were calculated by one-way ANOVA followed by the Tukey's *post hoc* test. Significant difference relative to Ctrl: $^{*}p<0.05$, $^{**}p<0.01$, $^{***}p<0.001$; significant difference relative to BB: $^{\#}p<0.05$, $^{\#\#}p<0.01$, $^{\#\#\#}p<0.001$.) BV/TV, the ratio of bone volume to the entire volume of the osteotomy; TMD, tissue mineral density; Tb.Th, trabecular thickness; Tb.N, trabecular number.

PS, and SP groups, and signs of corticalization were evident in the XP and SP groups (Fig. 4B).

Histomorphometric assessments

At day 14, the defects were filled with a significantly higher amount of newly formed bone in the PS and SP groups relative to controls, and in the XP group relative to the BB group only. All bioactive molecule-treated groups demonstrated significantly higher defect fill relative to the Ctrl group at day 28 (Fig. 5A).

Osteoblasts were significantly increased in the SP group relative to the BB group at day 14 ($p<0.05$, Fig. 5B). On the other hand, at day 14, TRAP(+) cells were significantly increased relative to the BB group ($p<0.05$ in XP, SB, and PS groups; $p<0.01$ in SP group; Fig. 5C). At day 28, osteoblasts appeared to be decreased in all investigated groups (Fig. 5B), and significantly increased TRAP(+) cells were noted in the XP and SP groups compared with the BB group ($p<0.05$, Fig. 5C).

Discussion

To maximize regeneration, the coordination of host cells, signaling molecules, and a scaffold with sufficient blood supply are all required.[2] More specifically, controlling the signaling molecules—such as growth factors or bioactive molecules to take action at the appropriate timing in a stabilized environment—is necessary to restore the dentoalveolar apparatus. Toward this end, we developed the dual-compartmental microsphere as a filler to maintain and stabilize the osteotomy site,[15] and this microsphere was also able to carry and control the release profile of two types of bioactive molecules (i.e., PDGF and simvastatin).[12] Whereas the promotion of osteogenesis in heat-damaged tissue has been demonstrated in our previous short-term study,[15] in the present investigation, we further validated the therapeutic efficacy of this combinatorial modality. Given that sequential PDGF–simvastatin release was able to accelerate dentoalveolar osteogenesis and maturation compared with the single bioactive molecule or parallel PDGF–simvastatin release groups (XP, SB, and PS groups) at day 14, and the single bioactive molecule-treated groups (XP and SB groups) demonstrated significantly greater osteogenesis compared with controls at day 28, this study confirmed the regeneration capability of PDGF and simvastatin and provided evidence of the acceleration of regeneration through the combination of bioactive molecules.

Based on the understanding of the bone-healing process, bone regeneration is timely and orderly regulated by the events of chemotaxis, cell proliferation, matrix synthesis, and differentiation.[18,19] As a potent mitogen and chemoattractant, PDGF promoted cell recruitment to accelerate wound healing and served as a stimulator of subsequent angiogenesis,[20] which not only introduced nutrients, but also made the cells capable of osteogenic differentiation.[21] As PDGF was not directly involved in the differentiation

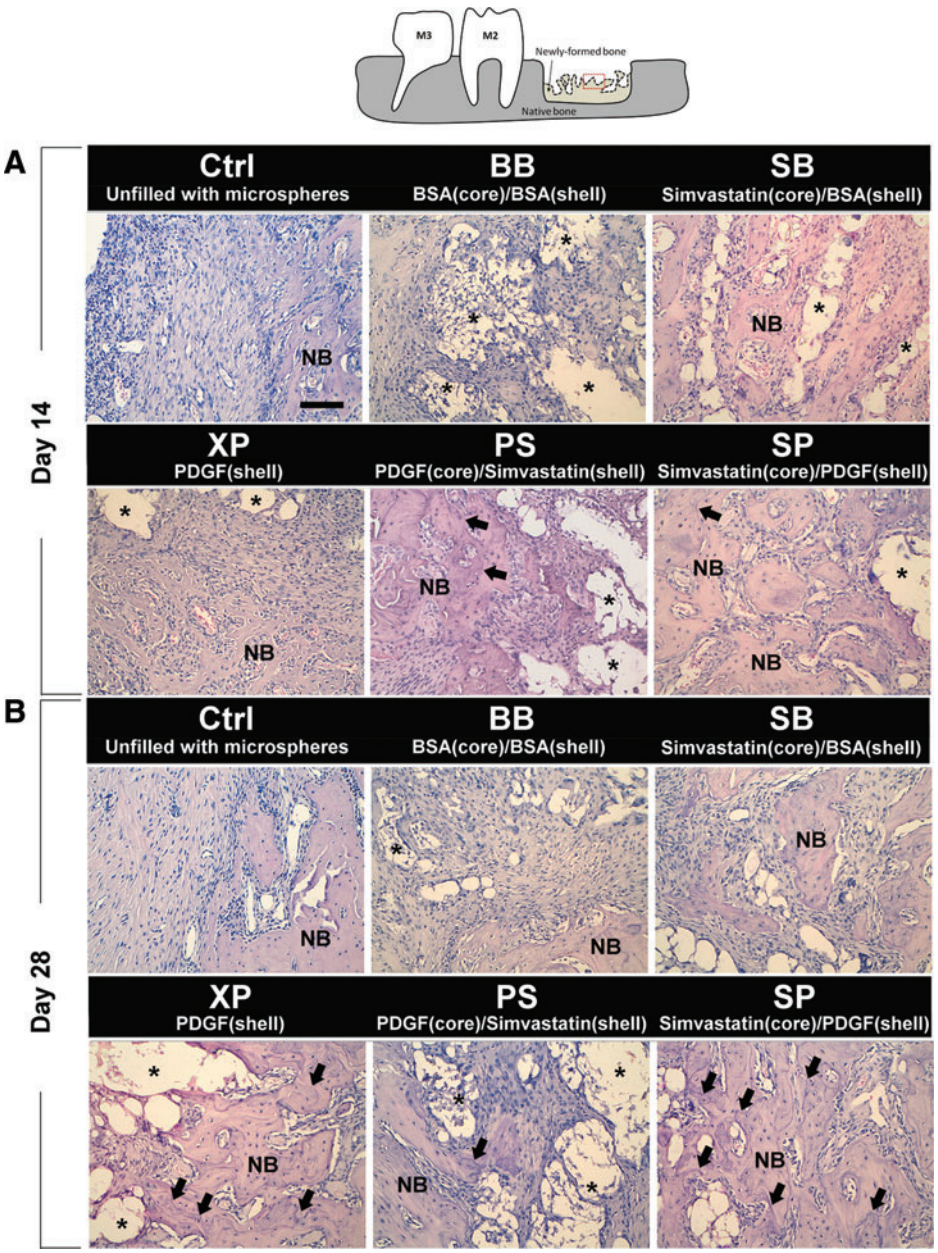

FIG. 4. Histological observations. The image was selected from the center of the osteotomy (dashed box in the upper panel) in a representative section of each group at **(A)** day 14 and **(B)** day 28. The asterisks indicate the residual microspheres, and the arrows indicate the reversal lines in the bone matrix (hematoxylin and eosin stain; magnification, 200×). M2, maxillary second molar; M3, maxillary third molar; NB, new bone. Color images available online at www.liebertpub.com/tea

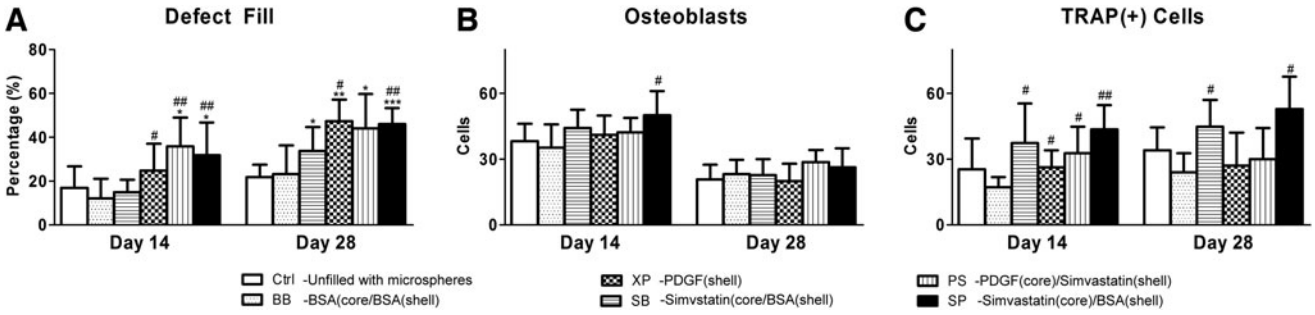

FIG. 5. Quantitative histological assessments. **(A)** The percentage of the defect filled with newly formed bone. **(B)** Numbers of osteoblasts within 25 micrometers from the surface of newly formed bone. **(C)** Numbers of TRAP(+) cells within 25 μm from the surface of newly formed bone. (Data are expressed as mean ± standard deviation, and differences between groups were calculated by one-way ANOVA followed by the Tukey's *post hoc* test. Significant difference relative to Ctrl: $^{*}p<0.05$, $^{**}p<0.01$, $^{***}p<0.001$; significant difference relative to BB: $^{\#}p<0.05$, $^{\#\#}p<0.01$, $^{\#\#\#}p<0.001$.) TRAP, tartrate-resistant acid phosphatase.

process, the modulation in the progression of osteogenesis might be limited. Thus, osteogenesis was apparently promoted at day 14 and gradually increased until day 28 in the XP group (Fig. 3), without significant alteration of the recruitment of the osteoblastic and osteoclastic cells (Fig. 5). Simvastatin, an inhibitor of 3-hydroxy-3-methylglutaryl coenzyme A (HMG-CoA) reductase, has been shown to upregulate the activities of BMP-2 and nitric oxide to induce *de novo* osteogenesis.[22] However, simvastatin appeared to only promote the proliferation of epithelial and endothelial cells[23,24] and might even inhibit the migration of fibroblastic cells[25] as well as the proliferation of smooth muscle cells.[26] Without the significant promotion of chemotaxis and mitogenesis, osteogenesis from simvastatin treatment was limited in the earlier stage. Conversely, simvastatin may augment angiogenesis to recruit cells for subsequent osteogenic differentiation (Fig. 3). Although the amount of newly formed bone may be limited in the SB group, slightly increased osteoblasts were noted at day 14 (Fig. 5B), and increased osteoclastic cells at both 14 and 28 days indicated that the bone maturation was still promoted (Fig. 5C). Taken together, PDGF recruited cells without the direct involvement of osteogenic differentiation, and simvastatin promoted osteogenic differentiation with limited effects on cell recruitment. As a consequence, both PDGF and simvastatin promoted osteogenesis under different mechanisms, and the maturation of bone appeared to be accelerated under simvastatin treatment. As such, the combination of PDGF and simvastatin to dually enhance the proliferative and differentiation phases of regeneration could be considered.

Our results demonstrated a significantly greater amount of osteogenesis with the initial union of bone from the border of the osteotomy in both the PS and SP groups at day 14 (Figs. 2, 3, and 5A). However, it appeared that osteogenesis in the PS group halted with a slight reduction of the TRAP lining after day 14 (Fig. 5). This may be because the persistent PDGF release in the PS group has interfered with the osteoinductive effect of simvastatin. Hseih and Graves reported the inhibition of osteogenic differentiation from continuous PDGF treatment, but short-term exposure did not inhibit the differentiated phenotype.[27] Marzouk *et al.* also indicated that osteogenic capabilities of the osteoblast progenitors were inferior while pretreated with PDGF, whereby short-term PDGF application was still effective in stimulating osteogenesis in calvarial defects.[28] Due to the minimal level of residual PDGF in the XP and SP groups in later stages, the inhibition of osteogenesis could be prevented, resulting in continuous bone growth and maturation at day 28 (Figs. 3 and 4). However, the osteoclastic cells were only significantly increased in the SP group (Fig. 5C), presumably associated with the differentiation potential of simvastatin.

The morphological patterns of osteogenesis were quantified by the three-dimensional micro-CT imaging of Tb.Th, Tb.Sp, and Tb.N, and those architectural parameters may reflect the dynamics and biomechanical strength of the bone.[29,30] The neogenic bone was characterized by increased numbers of thin trabeculae (primary spongiosa), and the bone trabeculae gradually thickened according to the deposition of bone matrix.[31] Unlike single bioactive molecule-treated groups (XP and SB groups), both Tb.N and Tb.Th were significantly increased in the PS and SP groups at day 14 (Fig. 3C, D), indicating that combined PDGF–simvastatin treatment may not only promote the initiation, but also accelerate the progression of osteogenesis. Reduced Tb.N was noted in the XP and SP groups at day 28, presumably due to the union of bone trabeculae upon bone matrix deposition, as characterized by the presentation of multiple reversal lines (Fig. 4B). A similar trend was noted in the histomorphometric measurement (Fig. 5A). However, in the PS group, BV/TV was apparently lower than the XP and SP groups at day 28, whereas such a distinction was not evident in the defect fill of histomorphometry. This phenomenon may attribute to the thinner and fewer bone trabeculae occupied in the marrow space (Fig. 3C, D). Corticalization within the osteotomy indicated that osteogenesis was complete[32] in the XP and SP groups at day 28, and a significantly higher ratio of lining osteoclasts in the SP group (Fig. 5C) implied that the newly formed bone was more mature compared with the XP group. Furthermore, the ~50% BV/TV of the osteotomy (Fig. 3A) indicated that full restoration of a large-sized osteotomy was not achievable, and further justification of the current mode is still necessary.

A dual-compartment microsphere composed of PDLLA and PLGA polymers was formulated to control the corelease profile of bioactive molecules. Both polymers are biocompatible and biodegradable polymers widely used in biomedical applications.[33] Using the CEHDA technique, our group has successfully fabricated double-layered PDLLA–PLGA microspheres, which simultaneously carried paclitaxel and suramin,[34] chitosan-p53 nanoparticles and doxorubicin,[35] and PDGF and simvastatin.[15] It is noteworthy that core-loaded molecules always achieved greater encapsulation efficiency than the shell-loaded molecules (Table 1), and this can be explained by the significant reduction of core-loaded molecule diffusion during the atomization process, whereas the jet instability caused by the outer emulsion phase may lead to the lower encapsulation efficiency of shell-loaded molecules.[12] According to the faster degradation nature of PLGA relative to PDLLA, the slower release rate of core-loaded relative to shell-loaded biomolecules, and the slower release rate of hydrophobic relative to hydrophilic molecules,[12] simvastatin (hydrophobic molecules in the core compartment consisting of PDLLA) was able to release more slowly than PDGF (hydrophilic molecules in the shell compartment consisting of PLGA) in the SP mode (Fig. 1E).

The clinical effective dose suggested by clinical studies was 1.2% w/w of simvastatin and 0.3 mg/mL of PDGF.[36,37] Due to the short half-lives and rapid diffusion profile, the majority of bioactive molecules did not contribute to the regeneration, and the high concentration of bioactive molecules in the peripheral tissue may also cause serious side effects.[38,39] Based on the calculation from our previous study,[15] the concentrations of PDGF and simvastatin delivered in the defect were about 1–1.5 $\mu g/mm^3$, relatively lower than the suggested clinical dose. The results from our study confirmed the controlled release property of the PDLLA–PLGA microspheres, and the dose utilized in this study was sufficient to promote dentoalveolar regeneration. However, the degraded products of the microspheres may elicit the production of inflammatory cytokines and retard the process of regeneration.[40,41] Inflammatory responses appeared to be suppressed and cellular viabilities were increased by the incorporation of PDGF or simvastatin.[12] On the other hand,

the higher and persistent PDGF expression may inhibit osteogenesis and even cause the fibrotic gingival hyperplasia,[27,42] whereas myopathy, glucose intolerance, and impaired renal function are the main concerns of taking simvastatin.[43,44] The therapeutic efficiency and the adverse effects of the dosage regimen of the microspheres are still yet to be confirmed.

The major limitation of this study is that the dentoalveolar defect was surgically created, and the nature, as well as the pattern of the defect, was not necessarily relevant to a deficient alveolar ridge in the clinical condition. However, preclinical validation of therapeutic efficacy in a standardized critical-sized defect is needed in the initial stages of investigation. Additionally, the resolution of inflammation and healing of rats appeared to be faster than in humans, potentially masking the influence of postoperative complications and overestimating the regeneration potential in humans.

Notwithstanding such limitations, the results from our study demonstrated that both PDGF and simvastatin augmented dentoalveolar osteogenesis, and sequential PDGF–simvastatin release from PDLLA–PLGA microspheres (SP group) is suggested according to the further accelerated osteogenesis and bone maturation. However, future investigations of the dosage regimen under more clinical relevant conditions are necessary to validate the efficacy of this combinational treatment modality.

Acknowledgments

This study was supported by research grants from NUS (R-221-000-034-133), National Medical Research Council of Singapore (R-221-000-028-275), and National Science Council of Taiwan (102-2314-B-002-003). The authors declare no conflicts of interest related to the study.

Disclosure Statement

No competing financial interests exist.

References

1. Retzepi, M., and Donos, N. Guided Bone Regeneration: biological principle and therapeutic applications. Clin Oral Implants Res **21,** 567, 2010.
2. Kaigler, D., Avila, G., Wisner-Lynch, L., Nevins, M.L., Nevins, M., Rasperini, G., *et al.* Platelet-derived growth factor applications in periodontal and peri-implant bone regeneration. Expert Opin Biol Ther **11,** 375, 2011.
3. Chang, P.C., Lang, N.P., and Giannobile, W.V. Evaluation of functional dynamics during osseointegration and regeneration associated with oral implants. Clin Oral Implants Res **21,** 1, 2010.
4. Wikesjo, U.M., Qahash, M., Huang, Y.H., Xiropaidis, A., Polimeni, G., and Susin, C. Bone morphogenetic proteins for periodontal and alveolar indications; biological observations—clinical implications. Orthod Craniofac Res **12,** 263, 2009.
5. Dereka, X.E., Markopoulou, C.E., and Vrotsos, I.A. Role of growth factors on periodontal repair. Growth Factors **24,** 260, 2006.
6. Schilephake, H. Bone growth factors in maxillofacial skeletal reconstruction. Int J Oral Maxillofac Surg **31,** 469, 2002.
7. Chen, L., Jiang, W., Huang, J., He, B.C., Zuo, G.W., Zhang, W., *et al.* Insulin-like growth factor 2 (IGF-2) potentiates BMP-9-induced osteogenic differentiation and bone formation. J Bone Miner Res **25,** 2447, 2010.
8. Patel, Z.S., Young, S., Tabata, Y., Jansen, J.A., Wong, M.E., and Mikos, A.G. Dual delivery of an angiogenic and an osteogenic growth factor for bone regeneration in a critical size defect model. Bone **43,** 931, 2008.
9. Hernandez, A., Reyes, R., Sanchez, E., Rodriguez-Evora, M., Delgado, A., and Evora, C. *In vivo* osteogenic response to different ratios of BMP-2 and VEGF released from a biodegradable porous system. J Biomed Mater Res A **100,** 2382, 2012.
10. Holland, T.A., Tabata, Y., and Mikos, A.G. Dual growth factor delivery from degradable oligo(poly(ethylene glycol) fumarate) hydrogel scaffolds for cartilage tissue engineering. J Control Release **101,** 111, 2005.
11. Raiche, A.T., and Puleo, D.A. *In vitro* effects of combined and sequential delivery of two bone growth factors. Biomaterials **25,** 677, 2004.
12. Chang, P.C., Chung, M.C., Lei, C., Chong, L.Y., and Wang, C.H. Biocompatibility of PDGF-simvastatin double-walled PLGA (PDLLA) microspheres for dentoalveolar regeneration: a preliminary study. J Biomed Mater Res A **100,** 2970, 2012.
13. Shah, P., Keppler, L., and Rutkowski, J. A review of platelet derived growth factor playing pivotal role in bone regeneration. J Oral Implantol 2012 [Epub ahead of print]; DOI: 10.1563/AAID-JOI-D-11-00173.1.
14. Mukozawa, A., Ueki, K., Marukawa, K., Okabe, K., Moroi, A., and Nakagawa, K. Bone healing of critical-sized nasal defects in rabbits by statins in two different carriers. Clin Oral Implants Res **22,** 1327, 2011.
15. Chang, P.C., Lim, L.P., Chong, L.Y., Dovban, A.S., Chien, L.Y., Chung, M.C., *et al.* PDGF-simvastatin delivery stimulates osteogenesis in heat-induced osteonecrosis. J Dent Res **91,** 618, 2012.
16. Burghardt, A.J., Kazakia, G.J., Laib, A., and Majumdar, S. Quantitative assessment of bone tissue mineralization with polychromatic micro-computed tomography. Calcif Tissue Int **83,** 129, 2008.
17. Bernhardt, A., Thieme, S., Domaschke, H., Springer, A., Rosen-Wolff, A., and Gelinsky, M. Crosstalk of osteoblast and osteoclast precursors on mineralized collagen—towards an *in vitro* model for bone remodeling. J Biomed Mater Res A **95,** 848, 2010.
18. Dimitriou, R., Tsiridis, E., and Giannoudis, P.V. Current concepts of molecular aspects of bone healing. Injury **36,** 1392, 2005.
19. Mistry, A.S., and Mikos, A.G. Tissue engineering strategies for bone regeneration. Adv Biochem Eng Biotechnol **94,** 1, 2005.
20. Cooke, J.W., Sarment, D.P., Whitesman, L.A., Miller, S.E., Jin, Q., Lynch, S.E., *et al.* Effect of rhPDGF-BB delivery on mediators of periodontal wound repair. Tissue Eng **12,** 1441, 2006.
21. Schipani, E., Maes, C., Carmeliet, G., and Semenza, G.L. Regulation of osteogenesis-angiogenesis coupling by HIFs and VEGF. J Bone Miner Res **24,** 1347, 2009.
22. Bradley, J.D., Cleverly, D.G., Burns, A.M., Helm, N.B., Schmid, M.J., Marx, D.B., *et al.* Cyclooxygenase-2 inhibitor reduces simvastatin-induced bone morphogenetic protein-2 and bone formation *in vivo*. J Periodontal Res **42,** 267, 2007.
23. Takahashi, S., Nakamura, H., Seki, M., Shiraishi, Y., Yamamoto, M., Furuuchi, M., *et al.* Reversal of elastase-induced pulmonary emphysema and promotion of alveolar epithelial

cell proliferation by simvastatin in mice. Am J Physiol Lung Cell Mol Physiol **294,** L882, 2008.
24. Wu, H., Jiang, H., Lu, D., Qu, C., Xiong, Y., Zhou, D., *et al.* Induction of angiogenesis and modulation of vascular endothelial growth factor receptor-2 by simvastatin after traumatic brain injury. Neurosurgery **68,** 1363, 2011; discussion 71.
25. Caceres, M., Romero, A., Copaja, M., Diaz-Araya, G., Martinez, J., and Smith, P.C. Simvastatin alters fibroblastic cell responses involved in tissue repair. J Periodontal Res **46,** 456, 2011.
26. Ali, O.F., Growcott, E.J., Butrous, G.S., and Wharton, J. Pleiotropic effects of statins in distal human pulmonary artery smooth muscle cells. Respir Res **12,** 137, 2011.
27. Hsieh, S.C., and Graves, D.T. Pulse application of platelet-derived growth factor enhances formation of a mineralizing matrix while continuous application is inhibitory. J Cell Biochem **69,** 169, 1998.
28. Marzouk, K.M., Gamal, A.Y., Al-Awady, A.A., and Sharawy, M.M. Platelet-derived growth factor BB treated osteoprogenitors inhibit bone regeneration. J Oral Implantol **34,** 242, 2008.
29. Alberich-Bayarri, A., Marti-Bonmati, L., Sanz-Requena, R., Belloch, E., and Moratal, D. *In vivo* trabecular bone morphologic and mechanical relationship using high-resolution 3-T MRI. AJR Am J Roentgenol **191,** 721, 2008.
30. Frost, H.M. On the trabecular "thickness"-number problem. J Bone Miner Res **14,** 1816, 1999.
31. Berglundh, T., Abrahamsson, I., Lang, N.P., and Lindhe, J. *De novo* alveolar bone formation adjacent to endosseous implants. Clin Oral Implants Res **14,** 251, 2003.
32. Cardaropoli, G., Araujo, M., and Lindhe, J. Dynamics of bone tissue formation in tooth extraction sites. An experimental study in dogs. J Clin Periodontol **30,** 809, 2003.
33. Anderson, J.M., and Shive, M.S. Biodegradation and biocompatibility of PLA and PLGA microspheres. Adv Drug Deliv Rev **28,** 5, 1997.
34. Nie, H., Fu, Y., and Wang, C.H. Paclitaxel and suramin-loaded core/shell microspheres in the treatment of brain tumors. Biomaterials **31,** 8732, 2010.
35. Xu, Q., Xia, Y., Wang, C.H., and Pack, D.W. Monodisperse double-walled microspheres loaded with chitosan-p53 nanoparticles and doxorubicin for combined gene therapy and chemotherapy. J Control Release **163,** 130, 2012.
36. Pradeep, A.R., Rao, N.S., Bajaj, P., and Kumari, M. Efficacy of subgingivally delivered simvastatin in the treatment of patients with type 2 diabetes and chronic periodontitis: a randomized double-masked controlled clinical trial. J Periodontol **84,** 24, 2013.
37. Nevins, M., Kao, R.T., McGuire, M.K., McClain, P.K., Hinrichs, J.E., McAllister, B.S., *et al.* Platelet-derived growth factor promotes periodontal regeneration in localized osseous defects: 36-month extension results from a randomized, controlled, double-masked clinical trial. J Periodontol **84,** 456, 2013.
38. Smith, D.M., Cooper, G.M., Mooney, M.P., Marra, K.G., and Losee, J.E. Bone morphogenetic protein 2 therapy for craniofacial surgery. J Craniofac Surg **19,** 1244, 2008.
39. Lauzon, M.A., Bergeron, E., Marcos, B., and Faucheux, N. Bone repair: new developments in growth factor delivery systems and their mathematical modeling. J Control Release **162,** 502, 2012.
40. Nicolete, R., dos Santos, D.F., and Faccioli, L.H. The uptake of PLGA micro or nanoparticles by macrophages provokes distinct *in vitro* inflammatory response. Int Immunopharmacol **11,** 1557, 2011.
41. Ji, W., Yang, F., Seyednejad, H., Chen, Z., Hennink, W.E., Anderson, J.M., *et al.* Biocompatibility and degradation characteristics of PLGA-based electrospun nanofibrous scaffolds with nanoapatite incorporation. Biomaterials **33,** 6604, 2012.
42. Subramani, T., Rathnavelu, V., and Alitheen, N.B. The possible potential therapeutic targets for drug induced gingival overgrowth. Mediators Inflamm **2013,** 639468, 2013.
43. Alla, V.M., Agrawal, V., Denazareth, A., Mohiuddin, S., Ravilla, S., and Rendell, M. A reappraisal of the risks and benefits of treating to target with cholesterol lowering drugs. Drugs **73,** 1025, 2013.
44. Larsen, S., Stride, N., Hey-Mogensen, M., Hansen, C.N., Bang, L.E., Bundgaard, H., *et al.* Simvastatin effects on skeletal muscle: relation to decreased mitochondrial function and glucose intolerance. J Am Coll Cardiol **61,** 44, 2013.

Address correspondence to:
Po-Chun Chang, DDS, PhD
Graduate Institute of Clinical Dentistry
School of Dentistry
National Taiwan University
1 Chang-Te Street
Taipei 100
Taiwan

E-mail: changpc@ntu.edu.tw

Received: November 20, 2012
Accepted: August 7, 2013
Online Publication Date: October 16, 2013